Delft University of Technology

Receiver Structures for Phase Modulated FMCW Radars

Kumbul, Utku; Petrov, Nikita; Vaucher, Cicero S.; Yarovoy, Alexander

Important note
To cite this publication, please use the final published version (if applicable).
Please check the document version above.

Receiver Structures for
Phase Modulated FMCW Radars

Utku Kumbul*, Nikita Petrov*, Cicero S. Vaucher†* and Alexander Yarovoy*
* Department of Microelectronics, Delft University of Technology, Delft, The Netherlands
† NXP Semiconductors, Eindhoven, The Netherlands
{u.kumbul, n.petrov, c.silveiravaucher, a.yarovoy}@tudelft.nl

Abstract—Two receiver structures of phase modulated FMCW signals with low ADC sampling requirement are investigated, namely the matched filter of the dechirped signal and the group delay filter approach. The sensing performance of the investigated receiver strategies are analyzed in application to BPSK modulated chirp. Numerical simulations demonstrate that both techniques provide comparable performance for low to moderate bandwidth of the modulation signal. Matched filter outperforms the group delay receiver for the modulation waveform with large bandwidth, hence with the price of larger computational complexity.

Index Terms—Modulated chirps, Filter bank, Group delay filter, Phase-coded FMCW, Joint sensing and communication.

I. INTRODUCTION

Radars are used for detection, tracking and classification under various weather conditions, and they are key sensors for the advanced driver-assistance systems (ADAS) to acquire self-awareness about the environment. Consequently, the number of radar-equipped vehicles on the road is predicted to grow in future and raise the spectral intensity [1]. To lower the spectral congestion, joint sensing and communication systems have become a notable alternative [2], and the variety of techniques have been investigated to achieve joint radar-communication (RadCom) coexistence [3]–[5]. One promising approach to realize this goal consists of modulating the conventional radar waveforms with the communication signals. Phase modulated continuous waveform and phase modulated FMCW waveforms have been proposed for this purpose, and research on multi-carrier waveforms is going on.

The linear frequency modulated continuous wave (LFMCW) waveform is widely used in automotive radars [6]. The FMCW excels in achieving high performance with a relatively low hardware complexity where the received signal is mixed with the transmitted signal to obtain the beat signal. The resulting beat signal contains information about the target and can be exploited to get range and velocity information by using the two-dimensional Fourier transform [7]. However, the FMCW is weak against mutual interference and not applicable for joint sensing and communication functionalities. This has motivated the idea of modulating FMCW signal with information signal in fast-time or slow-time.

Recently, the phase modulated FMCW have been used to overcome limitations of FMCW, such as providing joint sensing and communication [8]–[10]. In addition, the phase modulated FMCW is expected to enhance the robustness against radar to radar interference [11]. The matched filter for the full band signal in [12] and its approximation with group delay filter in [13] is used to process phase modulated FMCW. Since the automotive radar has limited processing power, it is imperative to find an effective processing method suitable to automotive radars.

In this paper, we investigate two receiving strategies for phase modulated FMCW signal suitable for automotive radars with low analog-to-digital converter (ADC) sampling requirements: the matched filter receiver applied to dechirped modulation signal and the group delay filter receiver. In order to accomplish this task, we recall the model and pre-processing of modulated LFMCW signal in Section II. Then in Section III we introduce and compare two aforementioned approaches to reconstruct the range profile from the received signal. The comparison study of two approaches and the impact of the waveform parameters on the radar performance are presented in Section IV. Furthermore, the measurement results that validate the investigated approaches are demonstrated in Section V. Finally, the conclusions are drawn in Section VI.

II. SIGNAL MODEL

Assume the radar transmits a wide-band LFM chirp modulated with a narrow-band modulation signal $m(t)$:

$$s_{\mathrm{t}}(t) = m(t)\exp\left(j2\pi\left(f_c t + \frac{\beta t^2}{2}\right)\right), \quad t \in [0, T], \quad (1)$$

where f_c stands for the carrier frequency of the radar, $\beta = B/T$ is the chirp rate, B and T are the bandwidth and the time duration of the chirp respectively.

The signal (1) impinges on a target at range r_0 moving with a constant radial velocity v_0 with respect to the radar. The reflected signal returns back to the radar with the time delay:

$$\tau_0(t) = \frac{2}{c}(r_0 + v_0 t) = \tau_0 + \frac{2v_0}{c}t \qquad (2)$$

and attenuated proportionally to the target RCS and two-way propagation of the way by the complex coefficient α_0. Then the received signal can be given by:

$$s_{\mathrm{r}}(t) = \alpha_0 s_{\mathrm{t}}(t - \tau_0(t))$$
$$\approx \alpha_0 m(t - \tau_0)\exp\left(j2\pi\left(f_c t - f_D t + \frac{\beta}{2}\left(t^2 - 2t\tau_0\right)\right)\right),$$
$$(3)$$

where we assumed $v_0 \ll c$ and denote $f_D = \frac{2v_0 f_c}{c}$. Moreover, target migration within each sweep is assumed negligible $m\left(t - \tau_0(t)\right) \approx m\left(t - \tau_0\right)$. Hereinafter we incorporate all the constant terms into α_0 for notation simplicity. Applying the dechirping (deramping) to the received signal by multiplying it with the transmitted chirp and filtering out carrier frequency components gives:

$$
\begin{aligned}
s_{\mathrm{b}}(t) &= s_{\mathrm{r}}(t)\exp\left(-j2\pi\left(f_c t + \frac{\beta t^2}{2}\right)\right) \\
&\approx \alpha_0 m\left(t - \tau_0\right)\exp\left(-j2\pi\left(\beta\tau_0 + f_D\right)t\right) \\
&\approx \alpha_0 m\left(t - \tau_0\right)\exp\left(-j2\pi f_b t\right),
\end{aligned}
\tag{4}
$$

where $f_b = \beta\tau_0 + f_D \approx \beta\tau_0$ is the beat frequency. The dechirped signal contains two main components: the delayed modulated signal and a tone at the beat frequency. The second item is standard for dechiping of LFM signals. It also comprises Doppler frequency shift due to target motion, which is typically negligible compared to the frequency resolution of the beat signal after applying FFT to it, i.e. $f_D \ll f_s/N$, where f_s is the sampling frequency of the beat signal and N is the number of fast-time samples.

III. SIGNAL PROCESSING

A. Filter bank receiver

The form of (4) can be alternatively interpreted if we denote $f_{VD} = \beta\tau_0$ as a virtual Doppler frequency shift. In this formulation it resembles the response of a general waveform $m(t)$ with the time delay τ_0 and Doppler frequency shift f_{VD}. Note that by definition f_{VD} is of the same order of magnitude as the bandwidth of the modulation signal $m(t)$. In this case, the optimal receiver in white noise is a matched filter for each range-Doppler hypothesis jointly [7]. It can be realized either via a filter bank for all possible range-Doppler hypothesis or via performing Doppler processing prior to range compression (if f_{VD} and τ were independent unknown parameters). Here $f_{VD} = \beta\tau_0$, thus the filter bank should be done only in range dimension. A similar approach called compensated stretch processing was earlier discussed in [10]. The receiver then performs:

$$
\begin{aligned}
y(\tau) &= \int_0^T s_{\mathrm{b}}(t)m^*\left(t - \tau\right)\exp\left(j2\pi\beta\tau t\right)dt \\
&= \int_0^T s_{\mathrm{b}}^*(t)m\left(t - \tau\right)\exp\left(-j2\pi\beta\tau t\right)dt,
\end{aligned}
\tag{5}
$$

where $(\cdot)^*$ denotes the complex conjugate. The received (complex) beat signal sampled by analog-to-digital converter (ADC) operating at the sampling frequency f_{s} is stored in vector $\mathbf{s} \in \mathbb{C}^{N\times 1}$, defined by:

$$
\mathbf{s} \approx \alpha_0 m\left(n/f_s - \tau_0\right)\exp\left(-j2\pi\beta\tau_0 n/f_s\right),
\tag{6}
$$

where $t = n/f_s, n = 0, \ldots, N - 1$.

The second part of the integral in (5) for the fixed τ can be given via a Hadamard product of two vectors $\mathbf{a}(\tau) \odot \mathbf{m}(\tau)$:

$$
\begin{aligned}
\mathbf{a}(\tau) &= \exp\left(-j2\pi\beta\tau n/f_s\right), \\
\mathbf{m}(\tau) &= m\left(n/f_s - \tau\right),
\end{aligned}
\tag{7}
$$

with $n = 0, \ldots, N - 1$, $\mathbf{a}(\tau), \mathbf{m}(\tau) \in \mathbb{C}^{N\times 1}$.

Stacking the steering vectors of beat signal and delayed modulation signal as columns in $N \times N_r$ matrices $\mathbf{A} = [\mathbf{a}(\tau_0), \ldots, \mathbf{a}(\tau_{N_r})]$ and $\mathbf{M} = [\mathbf{m}(\tau_0), \ldots, \mathbf{m}(\tau_{N_r})]$ with N_r being the predefined number of range cells in the range grid, it is possible to write the convolution (5) via a vector product:

$$
\mathbf{y} = \left(\mathbf{A} \odot \mathbf{M}\right)^H \mathbf{s}
\tag{8}
$$

Note that the conventional FMCW processing (with no extra modulation) can be equivalently shown considering $\mathbf{M} = \mathbf{1}^{N\times N_r}$.

In a real system operating with real (not complex) signals, down-conversion (3) should be followed by the low-pass filter to remove high-frequency components. In case of $m(t)$ being a signal with large power outside the main-beam, as it is for binary phase shift keying (BPSK) sequence with the bandwidth comparable to f_s, then the binary signal before and after filtering will be significantly different. That will lead to the distortion of the range profile. This can be compensated by filtering the reference modulation signal $m(t)$ with the same low-pass filter prior to applying it in (8). That will significantly reduce range profile distortion due to signal mismatch.

B. Group delay filter receiver

The range information of the target is embedded in the beat signal and it can be obtained by applying FFT. However, the modulation signal $m(t - \tau_0)$ should be removed from the dechirped signal before extracting the range information via FFT. For a short-range radar application $m(t - \tau_0) \approx m(t)$, then the dechirped signal can be demodulated by multiplying (4) with $m^*(t)$ directly [14]. However, the applicability of this processing is limited to the short range applications with $R_{\max} \le c/(2B_m)$, where B_m is the bandwidth of modulation signal $m(t)$. For applications where the aforementioned range requirement can not be satisfied, then the responses in all the range cells should be aligned in fast-time before demodulation to compensate the time delay τ_0. This alignment can be realized via the group delay filter as proposed in [13].

Consider a group delay filter with unity magnitude response as:

$$
H(f) = \exp\left(j\theta(f)\right),
\tag{9}
$$

where the filter has the group delay $\tau_{\mathrm{gr}}(f)$ and the phase delay $\tau_{\mathrm{ph}}(f)$. The group delay is the time delay of the narrow-band signal at a chosen frequency and is equals to the first derivative of the filter phase response. For proper demodulation of $m(t - \tau_0)$, the filter should eliminate the delay τ_0. Thus the required linear group delay is:

$$
\tau_{\mathrm{gr}}(f) = -\frac{1}{2\pi}\frac{d\theta(f)}{df}\bigg|_{f=f_b} = -f_b/\beta.
\tag{10}
$$
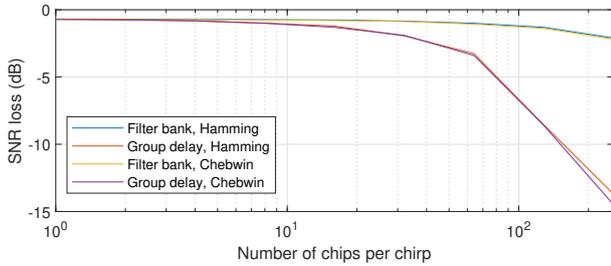
Fig. 1. SNR loss vs number of chips per chirp
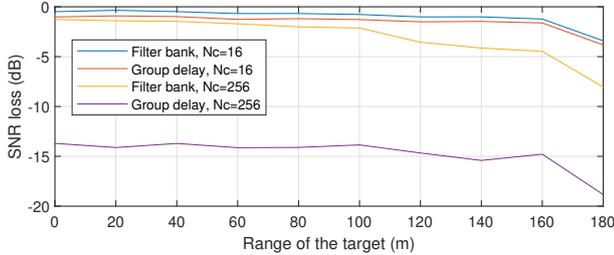
Fig. 2. SNR loss vs range of the target

Taking the integral of (10), the phase response of the group delay filter $H(f)$ becomes:

$$\theta(f) = \frac{\pi f^2}{\beta}. \tag{11}$$

The derived filter is applied to the dechirped signal in frequency domain, followed by demodulation in fast-time, which yields the response [13]:

$$\begin{aligned} y_o(t) &= \mathcal{F}^{-1}\{\mathcal{F}\{s_b(t)\}H(f)\}m^*(t) \\ &= \alpha_0 \exp\left(-j2\pi f_b t\right) \exp\left(j\epsilon(t)\right). \end{aligned} \tag{12}$$

Note that the group delay filter eliminated τ_0 for each beat signal and allows demodulation at ranges $R_{\max} \geq c/(2B_m)$. The derived filter has a quadratic frequency component within its phase response. Consequently, the filter leads to so-called group delay dispersion effect expressed via the residual phase error $\exp\left(j\epsilon(t)\right)$. For a narrow-band modulation signal with the bandwidth $B_m \ll f_s$, the residual phase error can be neglected. However, the narrow-band assumption can not be applied if B_m is comparable to f_s which will lead to the distortion of range response as demonstrated in the next section.

IV. PERFORMANCE ASSESSMENT

In this section, we compare the sensing performance of the signal processing described above. Assume an automotive radar transmitting phase modulated FMCW at carrier frequency $f_c = 77$ GHz with chirp duration $T = 12.6$ μs, and chirp bandwidth $B = 200$ MHz. The dechirped signal (4) is filtered by Hamming low-pass filter (LPF), if not mentioned otherwise, with the cut-off frequency $f_{cut} = \pm 20$ MHz. The sampling frequency for the beat signal is $f_s = 40$ MHz. For Doppler processing, $N_p = 32$ number of pulses is considered.
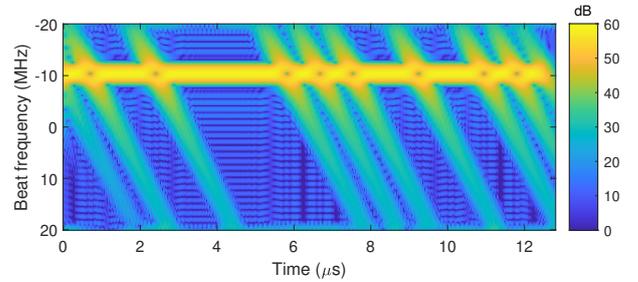
Fig. 3. Spectrogram of group delay filter output for $N_c = 16$

The modulation signal $m(t)$ is selected as random BPSK sequence with $m(t) \in \{-1, 1\}$. The bandwidth of the modulation signal B_m is controlled with the number of chips per chirp N_c as $B_m = N_c/T$. E.g. a modulation signal with a $N_c = 256$ has a bandwidth $B_m = 20$ MHz. To prevent signal mismatch, we apply the same LPF to the modulation signal used for demodulation in both receivers.

To focus on the waveform sensing properties, we consider a noise free scenario with a single target at the range $R_0 = 100$ m and the radial velocity $v_0 = 20$ m/s.

First, we investigated the signal-to-noise (SNR) loss versus number of chips per chirp for both processing approaches in Figure 1. For a long code, the bandwidth of the modulation signal becomes large and the LPF suppresses some parts of the signal, which lead to common for both receivers SNR loss. For comparison, we also considered LPF with Chebyshev window and noticed that the type of LPF has minor effect on the SNR loss (Figure 1).

Next, we illustrated the SNR loss as the function of the target range in Figure 2. As the beat frequency (proportional to target range) approaches to the cut-off frequency of the LPF, a part of the spectrum of the modulated signal is filtered out, which lead to SNR loss. Moreover, the group delay filter receiver suffers from huge residual phase error when the bandwidth of the modulation signal increases. This can be explained by the dispersion of BPSK signal due to the group delay filter. As shown in Figure 3, the BPSK signal has a wide spectrum in the time instances of the phase shifts, and the group delay filter applies different time delays to each frequency component. This leads to interference between adjacent phase shifts and degrades the demodulation performance. As a consequence, the range profile becomes distorted and can be seen as SNR loss in Figure 1 and Figure 2. The dispersion effect is more crucial for long code sequences (short time interval between chips).

For the selected radar parameters, the SNR loss is comparable up to $N_c = 16$ for both processing techniques while the SNR loss of the group delay method rapidly increases up to ~ 15 dB as the numbers of chips per chirp goes $N_c = 256$. This SNR loss behaviour can be seen in Figure 4 where the range profiles of both processing methods are compared for different number of chips per chirp. It can be observed that in the vicinity of the target, the response follows the Sinc-like
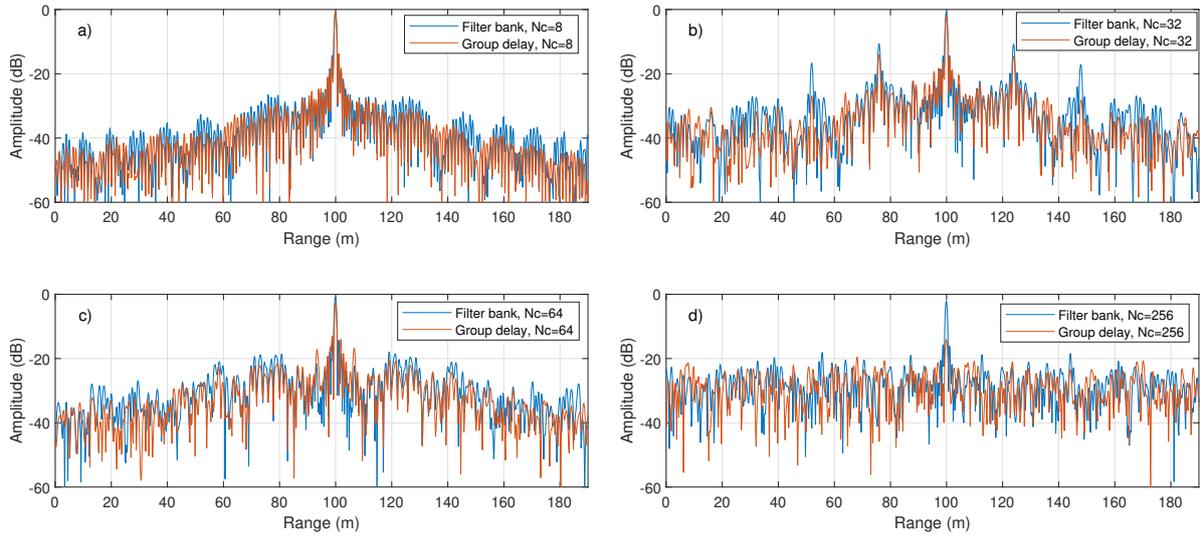
Fig. 4. Comparison of the range profile for both processing approaches

shape, expected for LFM processing. This region is defined by the main-beam width of the modulation $m(t)$. Outside of this region, the response has a noise-like pattern, typical for a random BPSK sequence. The level of this noisy sidelobe is determined by the time-bandwidth product of the modulation sequence, i.e. $-10 \log_{10}(TB_m)$ for each modulated chirp. It can be seen in Figure 4, the group delay filter approach has lower sidelobes compared to the filter bank approach in case of a small number of chips per chirp. However, the matched filter provides better performance for the long code sequences as it still recovers the mainlobe properly.

To assess the sidelobe level, we compared the integrated sidelobe level (ISL) for both processing methods defines as [15]:

$$ISL = 10 \log_{10} \left(\frac{\int_{-\infty}^{a} |y(f_d, \tau)|^2 d\tau + \int_{b}^{\infty} |y(f_d, \tau)|^2 d\tau}{\int_{a}^{b} |y(f_d, \tau)|^2 d\tau} \right),$$
(13)

where the interval $[a, b]$ contains the energy of the main lobe, and y is the signal for a given Doppler value f_D.

The ISL of the investigated processing methods are compared and demonstrated versus the number of chips per chirp in Figure 5. It is observed that the ISL of the group delay filter method up to the number of chips per chirp $N_c = 64$

is slightly lower compared to the filter bank approach. This is expected as the group delay filter method has lower sidelobes and similar SNR loss for a small number of chips per chirp, while the range profile of both processing methods looks very similar for a $N_c = 64$. However, the filter bank approach provides better SNR with a comparable sidelobe level as the number of chips per chirp increases, and thus the ISL of the group delay method becomes higher for the number of chips per chirp $N_c > 64$ as shown in Figure 5.

Finally, we investigated the range-Doppler profiles of both processing methods. The number of chips per chirp is selected as $N_c = 64$ since both methods have similar ISL values.
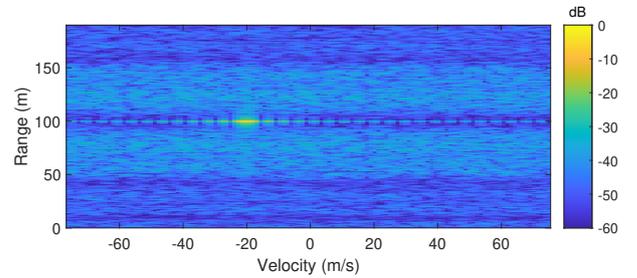
Fig. 6. Filter bank approach, range-Doppler profile for $N_c = 64$

Fig. 5. Comparison of the integrated sidelobe level vs number of chips per chirp for both processing techniques
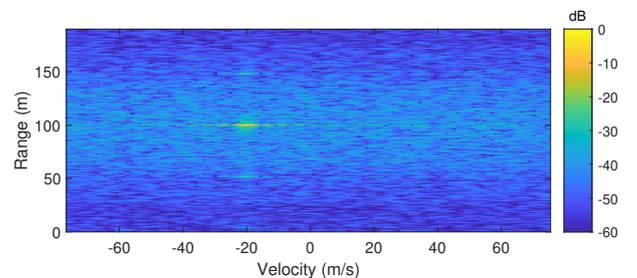
Fig. 7. Group delay filter approach, range-Doppler profile for $N_c = 64$
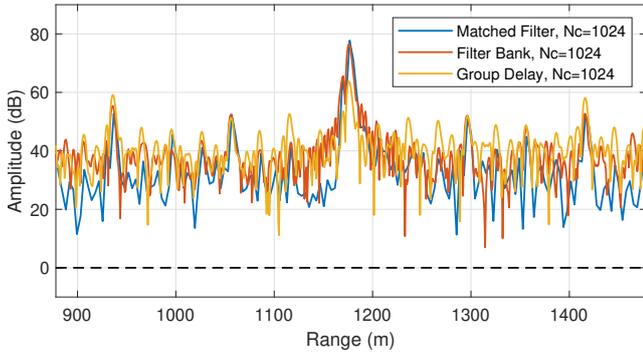
Fig. 8. Moving target experiment; Comparison of the range profile for the three processing approaches

The range-Doppler profiles are demonstrated in Figure 6 and Figure 7 for filter bank and group delay methods, respectively. Both figures show that the investigated processing methods detect the moving target at -20 m/s. Note that the group delay filter approach uses FFT, and therefore it has the computational complexity of $\mathcal{O}(N_c \log_2(N_c))$ where the filter bank method uses DFT which has the $\mathcal{O}(N_c^2)$ as computational complexity.

V. Experiments

The experimental assessment of the investigated processing approaches has been done using PARSAX, which is an S-band polarimetric Doppler radar. We have transmitted phase modulated FMCW at carrier frequency $f_c = 3.315$ GHz with chirp duration $T = 1$ ms, and chirp bandwidth $B = 40$ MHz. The modulation signal $m(t)$ is selected as zero correlation-zone (ZCZ) code family and we set number of chips per chirp $N_c = 1024$. Thus, the modulation signal has a bandwidth $B_m = 1.024$ MHz. Moreover, we transmitted $N_p = 128$ chirps with identical codes for Doppler processing.

During measurements, we observe a moving car located at 1178 m away from the radar with a radial velocity ~ 15 m/s. We have applied two investigated processing approaches to the collected data. In addition, we have performed full-band matched filtering as discussed in [14] for comparison with. The range profiles estimated with approaches are compared and demonstrated in Figure 8. The noise level is estimated from another target-free Doppler cell and used to normalize the signal power (represented as a black dashed line). The group delay filter approach suffers from residual phase error that leads to the high SNR loss for a long code sequence, as demonstrated in Figure 1. The full-band matched filter and the filter bank approaches provide similar range profiles, and both of them outperform the group delay filter approach for this long code sequence scenario.

VI. Conclusion

The phase modulated chirp signal with a joint sensing and communication capability has been investigated. We have analyzed filter bank and group delay filter receivers with low ADC sampling requirements suitable for automotive radar.

The trade-off between sensing performance and the information capacity of the waveform is demonstrated for both processing methods. It is shown that both processing receiver structures give comparable range profiles for short to moderate bandwidth of the modulation signal, while the filter bank approach provides favorable performance as the number of chips increases.

References

[1] M. Kunert, H. Meinel, C. Fischer, and M. Ahrholdt, "Report on interference density increase by market penetration forecast," in *MOSARIM Consortium, CNTR, Tech. Rep. D1.6, Sep.*, 2010.

[2] F. Liu, C. Masouros, A. Petropulu, H. Griffiths, and L. Hanzo, "Joint radar and communication design: Applications, state-of-the-art, and the road ahead," *IEEE Transactions on Communications*, vol. 68, pp. 3834–3862, 2020.

[3] S. A. Hassani, A. Guevara, K. Parashar, A. Bourdoux, B. van Liempd, and S. Pollin, "An in-band full-duplex transceiver for simultaneous communication and environmental sensing," in *2018 52nd Asilomar Conference on Signals, Systems, and Computers*, 2018, pp. 1389–1394.

[4] R. M. Gutierrez, H. Yu, A. R. Chiriyath, G. Gubash, A. Herschfelt, and D. W. Bliss, "Joint sensing and communications multiple-access system design and experimental characterization," in *2019 IEEE Aerospace Conference*, 2019, pp. 1–8.

[5] M. F. Keskin, R. F. Tigrek, C. Aydogdu, F. Lampel, H. Wymeersch, A. Alvarado, and F. M. J. Willems, "Peak sidelobe level based waveform optimization for ofdm joint radar-communications," in *2020 17th European Radar Conference (EuRAD)*, 2021, pp. 1–4.

[6] I. Bilik, O. Longman, S. Villeval, and J. Tabrikian, "The rise of radar for autonomous vehicles: Signal processing solutions and future research directions," *IEEE Signal Processing Magazine*, vol. 36, no. 5, pp. 20–31, 2019.

[7] M. I. Skolnik, *Radar handbook*. McGraw-Hill Education, 2008.

[8] S. D. Blunt, M. Cook, J. Jakabosky, J. De Graaf, and E. Perrins, "Polyphase-coded fm (pcfm) radar waveforms, part i: implementation," *IEEE Transactions on Aerospace and Electronic Systems*, vol. 50, no. 3, pp. 2218–2229, 2014.

[9] D. Schindler, B. Schweizer, C. Knill, J. Hasch, and C. Waldschmidt, "Mimo-ofdm radar using a linear frequency modulated carrier to reduce sampling requirements," *IEEE Transactions on Microwave Theory and Techniques*, vol. 66, no. 7, pp. 3511–3520, 2018.

[10] P. M. McCormick, C. Sahin, S. D. Blunt, and J. G. Metcalf, "FMCW implementation of phase-attached radar-communications (PARC)," in *2019 IEEE Radar Conference (RadarConf)*, 2019, pp. 1–6.

[11] F. Uysal, "Phase-coded fmcw automotive radar: System design and interference mitigation," *IEEE Transactions on Vehicular Technology*, vol. 69, no. 1, pp. 270–281, 2020.

[12] J. Reneau and R. R. Adhami, "Phase-coded LFMCW waveform analysis for short range measurement applications," in *2014 IEEE Aerospace Conference*, 2014, pp. 1–6.

[13] F. Lampel, R. F. Tigrek, A. Alvarado, and F. M. J. Willems, "A performance enhancement technique for a joint FMCW RadCom system," in *2019 16th European Radar Conference (EuRAD)*, 2019, pp. 169–172.

[14] U. Kumbul, N. Petrov, F. van der Zwan, C. S. Vaucher, and A. Yarovoy, "Experimental investigation of phase coded fmcw for sensing and communications," in *2021 15th European Conference on Antennas and Propagation (EuCAP)*, 2021, pp. 1–5.

[15] M.-E. Chatzitheodoridi, A. Taylor, and O. Rabaste, "A mismatched filter for integrated sidelobe level minimization over a continuous doppler shift interval," in *2020 IEEE Radar Conference (RadarConf20)*, 2020, pp. 1–6.